Title

Rationally Designed 2D Covalent Organic Framework with a Brick-Wall Topology

Journal

ACS Macro Letters, 5(12)

ISSN

2161-1653

Authors

Cai, Song-Liang

Zhang, Kai

Tan, Jing-Bo

et al.

Publication Date

2016-12-20

DOI

10.1021/acsmacrolett.6b00805

Peer reviewed

A Rationally Designed 2D Covalent Organic Framework with a Brick-Wall Topology

Song-Liang Cai,[†] Kai Zhang,[†] Jing-Bo Tan,[&] Sha Wang,[†] Sheng-Run Zheng,*[†] Jun Fan,[†] Ying Yu,[†] Wei-Guang Zhang*[†] and Yi Liu*[‡]

[†]School of Chemistry and Environment, South China Normal University, Guangzhou 510006, P. R. China

[‡]The Molecular Foundry, Lawrence Berkeley National Laboratory, Berkeley, California 94720, United States

[&]School of Chemistry and Chemical Engineering, Sun Yat-Sen University, Guangzhou, 510275, P. R. China

Supporting Information Placeholder

ABSTRACT: We report the design and synthesis of an imine-based two-dimensional covalent organic framework (2D COF) with a novel brick-wall topology by judiciously choosing a tri-topic T-shaped building block and a ditopic linear linker. Unlike the main body of COF frameworks reported to-date, which consists of higher-symmetry 2D topologies, the unconventional layered brick-wall topology have only been proposed but never been realized experimentally. The brick-wall structure was characterized by powder X-ray diffraction analysis, FT-IR, solid state ^{13}C NMR spectroscopy, nitrogen and carbon oxide adsorption−desorption measurements as well as theoretical simulations. Our present work opens the door to the design of novel 2D COFs and will broaden the scope of emerging COF materials.

Covalent organic frameworks (COFs),[1] which represent an emerging class of porous crystalline polymers with well-defined two- or three-dimensional structures, have received significant attention in the fields of materials chemistry in recent years, owing not only to their unique topological structures, but also to their diverse potential applications in gas storage,[2] heterogeneous catalysis,[3] chemical sensors,[4] photoelectric devices,[5] to name a few. Since the pioneering work of Yaghi and co-workers in 2005,[1a] a great number of crystalline COFs with interesting structures and useful properties have been successfully synthesized based on different types of reversible organic reactions such as boronate ester formation,[1a, 2c, 6] boronic acid trimerization,[1a, 7] nitrile trimerization,[8] nitroso self-addition,[9] imidization,[10] Schiff base[3, 4, 11] and hydrazone reactions.[12]

The structures of COF materials, to some extent, are predictable and predesignable because their skeleton topologies are mainly dependent on the geometry of the organic building blocks employed in the condensation reactions.[1] Taking the two-dimensional (2D) COF structures as examples, the first COF material COF-5, which displays a honeycomb-like topological structure, can be built by the reaction of a trigonal building block with a linear building block (Scheme 1a).[1a] The combination of a tetragonal building block with a linear linker, on the other hand, gives rise to 2D COF structures with a tetragonal topology (Scheme 1b).[6b] Additionally, when a linear linker is subjected to react with a hexagonal building block, the 2D COF structure with a triangular topology can be successfully achieved (Scheme 1c).[11f] It is noteworthy to mention that the most reported 2D COF materials are constructed based on the above-mentioned trigonal, tetragonal, or hexgonal building blocks, with some structural variants such as desymmetrized vertex designed building blocks.[11g] Unconventional 2D COF topologies, such as these low-symmetry herringbone (Scheme 1d) or brick-wall networks (Scheme 1e), in principle can be assembled from T-shaped building blocks[13] but have never been realized experimentally.

Scheme 1. Construction of 2D COFs with (a) Hexagonal, (b) Tetragonal, (c) Trigonal, (d) Herringbone, and (e) Brick-Wall Topologies Based on Different Multitopic Organic Building Blocks (BBs = Building Blocks).

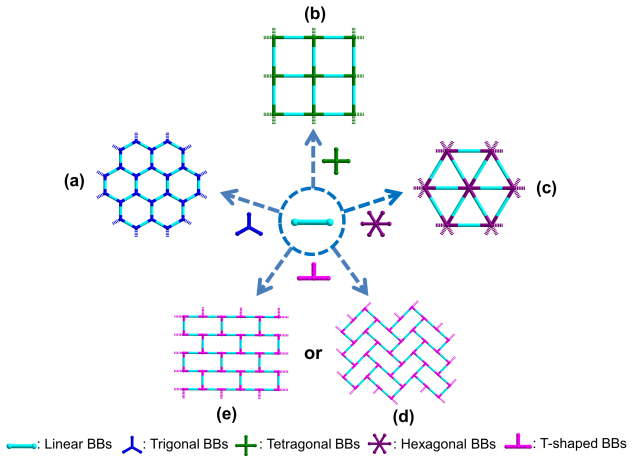

The combination of a T-shaped building block with a linear linker may theoretically produce a variety of possible networks, among which brick-wall and herringbone 2D COFs are the two most plausible ones as such topological structures have been frequently observed in the crystal structures of metal organic frameworks (MOFs).[14] Herein, we demonstrate the design, synthesis and characterization of an unprecedented 2D imine-based COF structure, termed brick-wall-COF, by employing a rigid T-shaped building block that contains three aldehyde groups. The brick-wall topology of the resulting COF is supported by powder X-ray diffraction analysis, detailed theoretical simulations, as well as nitrogen adsorption−desorption measurement.

Scheme 2. Schematic Representation of the Synthesis of the Brick-Wall-COF.

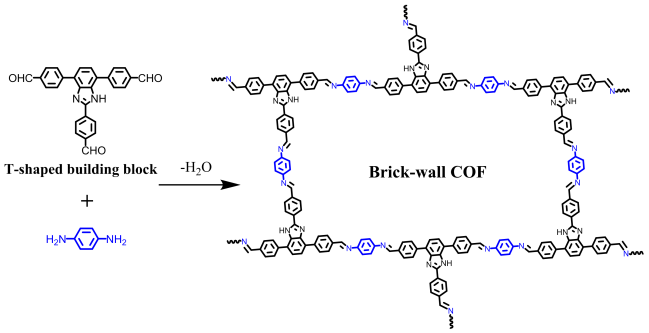

Since solvent has been demonstrated as one of the crucial factors on the construction of crystalline COF materials,[15] the synthesis of brick-wall COF was carried out by choosing various solvents (Figures S1-S2, Supporting Information). Dioxane was firstly employed as the solvent for the condensation reaction, the resulting powder however was identified to be the T-shaped building block, as evidenced by the powder X-ray diffraction (PXRD) measurements. When a good solvent of DMSO was mixed with dioxane at a ratio of 1/1 (v/v) and used for the reaction, all the diffraction peaks of T-shaped building block disappeared in the PXRD pattern, nevertheless, only two weak peaks could be observed, indicating a lack of long-range molecular ordering. A mixture of dioxane and mesitylene at a ratio of 1/1 was then employed for the condensation reaction, which resulted in weak diffraction peaks that corresponded to the T-shaped building block as well as intense signals in the smaller angle region, suggesting that COF material with relatively high crystallinity was formed but co-existed with unreacted T-shaped building block. The condensation reactions were further studied by increasing the relative amount of mesitylene in the mixed dioxane/mesitylene solvent system (Figure S2). Interestingly, when the ratio of dioxane to mesitylene was adjusted to 2/3, the resulting product showed two strong and several weak diffraction peaks, with complete disappearance of diffraction signals of the T-shaped building block. Further increase of the mesitylene content to a ratio of 1/3 or 1/9 all failed to the synthesis of the highly crystalline COF. Overall, at the optimal conditions, crystalline COF product could be prepared by reacting the T-shaped building block with 1,4-diaminobenzene in a degassed mixture of aqueous acetic acid (3M)/dioxane/mesitylene (1:4:6 v/v/v) at 110 °C for 72 h (Scheme 2 and S4) and isolated as a deep brown solid in a yield of 82%. Additionally, the T-shaped model compound (Scheme S3) was synthesized as pale yellow powder in 76% yield.

The synthesized brick-wall-COF was characterized employing different analytical techniques. The Fourier transform infrared (FT-IR) spectroscopy of the COF exhibits a medium strong C=N stretch around 1617 cm^{-1}, suggesting the formation of imine linkages. Such a C=N vibration band can also be observed in the FT-IR spectra of the T-shaped model compound. Meanwhile, compared with the FT-IR spectra of the starting materials 1,4-diaminobenzene and T-shaped building block, the amino (3150 − 3450 cm^{-1}) and aldehyde (1696 cm^{-1}) bands of the COF are significantly decrease (Figures S3-S7), also indicating the consumption of the two starting materials. ^{13}C cross-polarization magic-angle spinning (CP-MAS) solid-state NMR spectrum of the COF (Figure S9) presents a strong characteristic signal at 157.9 ppm, further confirming the formation of the expected imine C=N bonds. Additional five strong peaks at 149.1, 141.1, 136.2, 129.6, and 122.7 ppm can be ascribed to the carbon atoms of the phenyl and benzimidazolyl groups, whereas a weak signal at 194.2 ppm may be attributable to the carbon atoms of terminal aldehyde groups at the edges of the COF material.[3a] Thermogravimetric analysis (TGA) of the COF indicates a thermal stability up to 320 °C under nitrogen atmosphere (Figure S10). Environmental stability of the brick-wall-COF was also assessed in water, common organic solvents, aqueous acid and base, by soaking the COF samples in the corresponding solvents at room temperature for 24 hours. It was found that the brick-wall-COF was stable in water, hexane, MeOH, and THF, as their IR spectra remained unchanged after solvent treatment, but would degrade in HCl (12 M) and NaOH (12 M) solution (Figure S8). In addition, the scanning electron microscopy (SEM) image of the COF reveals a platelet morphology with edge length of several microns (Figure 1), which is consisted of nanoscale crystallites (Figures S11).

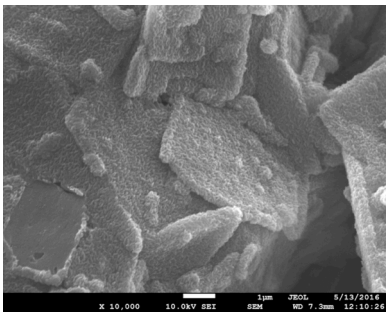

Figure 1. SEM image of brick-wall-COF showing the platelet morphology with edge length of several microns

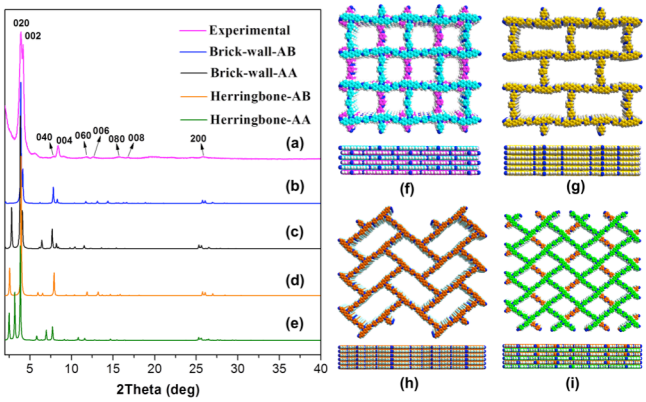

Figure 2. Experimental PXRD patterns of brick-wall-COF (a); Simulated PXRD patterns of brick-wall-COF: AB packing (b) and AA packing (c) structures; Simulated PXRD patterns of herringbone-COF: AB packing (d) and AA packing (e) structures; Space-filling models of brick-wall-COF: AB packing (f) and AA packing (g) structures; Space-filling models of herringbone-COF: AA packing (h) and AB packing (i) structures.

In order to better understand the crystalline structure of the resulting COF, framework models based on either brick-wall or herringbone topologies, which represent the two most plausible 2D extended structures, were built using *Materials Studio* software and the corresponding diffraction patterns were simulated. As illustrated in Figures 2a and 2b, the experimental PXRD pattern of brick-wall-COF displays two strongest diffraction peaks at 2θ = 3.90 and 4.18°, together with weaker peaks at 2θ = 7.82, 8.33, 11.83, 12.54, 15.77, 16.79, and 25.85°, which closely match those in the calculated patterns generated from the simulated structure based on a brick-wall network with AB packing (Figure 2f). The diffraction peaks can be assigned to the (020), (002),

(040), (004), (060), (006), (080), (008), and (200) facets, respectively. Based on this structure, Pawley refinement of the observed PXRD profiles using Reflex (implemented in *Materials Studio* software) was subsequently carried out to produce a PXRD pattern (Figure S12, dotted red curve) which was in great agreement with the experimental one, as evidenced by their negligible difference (Figure S12, green curve). The refinement results offer us a structure of the *Pmma* space group and a unit cell with parameters of a = 7.30 Å, b = 48.05 Å, c = 44.70 Å. The final wR_p and R_p values converged to 6.42% and 4.54%, respectively. In contrast, the calculated PXRD pattern from another brick-wall network structure with AA packing does not fit well with the experimental PXRD pattern (Figures 2c and 2g). For the COF model with the herringbone topology (Figures 2h and 2i), regardless of its packing geometries (eclipsed AA or staggered AB), the calculated PXRD patterns are not in agreement with the experimental one (Figures 2d and 2e). On the basis of these results, the resulting COF can be described as a 2D brick-wall network structure with AB packing (Figure 2f). Such an AB packing mode of COF is similar to that observed for COF-1.[1a]

The porous nature of brick-wall-COF was evaluated by nitrogen adsorption–desorption measurement at 77 K. Prior to porosity measurement, the synthesized sample was thermally activated at 150 °C and under a dynamic vacuum of 10^{-5} torr for 12 h. As illustrated in Figure 3a, the brick-wall-COF presented a reversible type IV sorption isotherm with a sharp nitrogen uptake under low relative pressures region ($P/P_0 < 0.1$), which is the typical characteristic for microporous materials. A surface area of 533 $m^2 g^{-1}$ could be calculated using the Langmuir model for P/P_0 between 0.10 and 0.30 (Figure S14). When employing the Brunauer–Emmett–Teller (BET) model ($0.005 < P/P_0 < 0.09$), the surface area value was determined to be 401 $m^2 g^{-1}$ (Figure S15), which is relatively low but comparable to that of the recently reported 2D COFs.[3a, 6d] The total pore volume was calculated to be 0.34 $cm^3 g^{-1}$ from a single point measurement at P/P_0 = 0.99. Such a relatively low BET surface area and total pore volume of brick-wall-COF is consistent with the fact that brick-wall-COF is packed in an AB mode rather than in an AA fashion. In addition, the porous structure of brick-wall-COF was further corroborated by fitting nonlocal density functional theory (NLDFT) using the carbon cylindrical pore adsorption branch mode (Figure 3b). The brick-wall-COF exhibited a narrow pore size distribution centered around 2.0 nm, which is consistent with the pore size estimated from the AB packing (1.7 – 2.2 nm, see Figure S13).

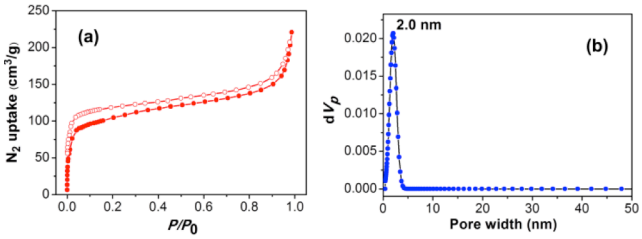

Figure 3. N_2 adsorption (●) and desorption (○) isotherm curves (a) and pore size distribution (b) of brick-wall-COF.

The as-synthesized brick-wall-COF material was further employed as the adsorbent for CO_2 capture by taking advantage of its unique feature of basic nitrogen groups deriving from the imine linkage and benzimidazole unit. The CO_2 adsorption isotherms of the brick-wall-COF were collected at different temperatures (298, 273 and 195 K) under 1.0 bar pressure, and the results were shown in Figure 4a. At the temperature of 298 and 273 K, the amounts of CO_2 uptake steadily increase with the increasing pressure and reach the maximum values of 21.4 and 39.5 mg g^{-1}, respectively. While the isotherm at 195 K displays an obvious two-step behavior,[16] of which the CO_2 uptake capacity exhibits a steep rise at low pressure, and then increases slowly at high pressure to reach a plateau of 404.3 mg g^{-1}. We also calculated the isosteric heat of adsorption (Q_{st}) for CO_2 using Clausius–Clapeyron equation (Figure 4b). The Q_{st} value at the onset of adsorption was found to be 37.49 kJ/mol, which then decreases and remains almoststable at 26 – 29 kJ/mol. Such a relatively high Q_{st} value is ascribable to the strong interactions between adsorbed CO_2 molecules and the Lewis basic imine and benzimidazole functionalities decorating the pores of brick-wall-COF material.[17] The selective uptake of CO_2 and N_2 has been investigated based on their corresponding sorption isotherm curves. On the basis of initial slope calculations[18] in the pressure range, the ideal adsorption selectivity of CO_2/N_2 is calculated to be 112 at 195 K and 68 at 273 K, respectively (Figures S16-S17). Such selectivity is comparable to the related 2D hexagonal COF material,[19] which may be contributed to strong interactions between N-H sites on the pore walls of brick-wall COF and the polarizable CO_2 molecules.

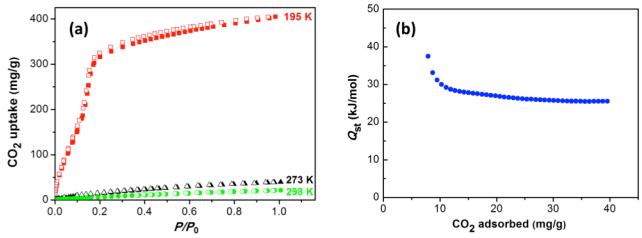

Figure 4. CO_2 adsorption (filled) and desorption (open) isotherms of the brick-wall-COF at 298 K, 273 K and 195 K (a); Enthalpy of adsorption plots as a function of the amount of CO_2 uptake (b).

In conclusion, we have successfully designed and synthesized a novel 2D COF with a hitherto unreported brick-wall topology from the condensation reaction between a linear diamine and a tri-topic T-shaped trisaldehyde building block under solvothermal conditions. The brick-wall framework structure of the resulting 2D COF has been well characterized by powder X-ray diffraction analysis, detailed theoretical simulations, as well as nitrogen adsorption–desorption measurement. Our results open up new perspectives towards the design of COFs with lower symmetry and unconventional topology, and hold great promises for the discovery of emerging COF materials through similar assembly schemes. We envision that new 2D COFs with brick-wall or herringbone topology packed in AA mode could be constructed with the proper choice of reaction conditions and T-shaped building blocks. These potentials are currently under investigation in our group.

ASSOCIATED CONTENT

Supporting Information.

The Supporting Information is available free of charge on the ACS Publications website at DOI: 10.1021/acsmacrolett.xxxxxxx.

Full synthetic procedure, IR spectra, solid-state ^{13}C NMR spectrum, SEM, TGA trace, LC-MS, PXRD analysis and coordinates of crystal structure models (PDF)

AUTHOR INFORMATION

Corresponding Author

*E-mail: yliu@lbl.gov

*E-mail: wgzhang@scnu.edu.cn
*E-mail: zhengsr@scnu.edu.cn

Notes

The authors declare no competing financial interest.

ACKNOWLEDGMENTS

S.L.C. is grateful to the NSFC (Grant No. 21603076), the Natural Science Foundation of Guangdong Province (Grant No. 2016A030310437) and the SCNU Foundation for Fostering Young Teachers (Grant No. 15KJ02). S.W. thanks the Undergraduates' Innovating Experimentation Project of SCNU (Grant No. hx201602). J.F. is supported by the Guangdong Provincial Science and Technology Project (Grant Nos. 2014A010101145 and 2016B090921005). S.R.Z., Y.Y., and W.G.Z. acknowledge the support from the NSFC (Grant Nos. 21473062, 21575043 and 21571070, respectively). Part of the work is carried out as a user project at the Molecular Foundry, which is supported by the Office of Science, Office of Basic Energy Sciences, of the U.S. Department of Energy under contract no. DE-AC02-05CH11231.

REFERENCES

1 (a) Cote, A. P.; Benin, A. I.; Ockwig, N. W.; O'Keeffe, M.; Matzger, A. J.; Yaghi, O. M. *Science* **2005**, *310*, 1166. (b) Feng, X.; Ding, X. S.; Jiang, D. L. *Chem. Soc. Rev.* **2012**, *41*, 6010. (c) Ding, S. Y.; Wang, W. *Chem. Soc. Rev.* **2013**, *42*, 548. (d) Colson, J. W.; Dichtel, W. R. *Nat. Chem.* **2013**, *5*, 453. (e) Waller, P. J.; Gandara, F.; Yaghi, O. M. *Acc. Chem. Res.* **2015**, *48*, 3053. (f) Cai, S. L.; Zhang, W. G.; Zuckermann, R. N.; Li, Z. T.; Zhao, X.; Liu, Y. *Adv. Mater.* **2015**, *27*, 5762. (g) Segura, J. L.; Mancheño, M. J.; Zamora, F. *Chem. Soc. Rev.* **2016**, DOI: 10.1039/c5cs00878f.

2 (a) Han, S. S.; Furukawa, H.; Yaghi, O. M.; Goddard, W. A. *J. Am. Chem. Soc.* **2008**, *130*, 11580. (b) Furukawa, H.; Yaghi, O. M. *J. Am. Chem. Soc.* **2009**, *131*, 8875. (c) Doonan, C. J.; Tranchemontagne, D. J.; Glover, T. G.; Hunt, J. R.; Yaghi, O. M. *Nat. Chem.* **2010**, *2*, 235. (d) Du,Y.; Yang, H. S.; Whiteley, J. M.; Wan, S.; Jin, Y. H.; Lee, S. H.; Zhang, W. *Angew. Chem., Int. Ed.* **2016**, 55, 1737.

3 (a) Ding, S. Y.; Gao, J.; Wang, Q.; Zhang, Y.; Song, W. G.; Su, C. Y.; Wang, W. *J. Am. Chem. Soc.* **2011**, *133*, 19816. (b) Fang, Q. R.; Gu, S.; Zheng, J.; Zhuang, Z. B.; Qiu, S. L.; Yan, Y. S. *Angew. Chem., Int. Ed.* **2014**, *53*, 2878. (c) Xu, H.; Gao, J.; Jiang, D. L. *Nat. Chem.* **2015**, *7*, 905.

4 (a) Dalapati, S.; Jin, S. B.; Gao, J.; Xu, Y. H.; Nagai, A.; Jiang, D. L. *J. Am. Chem. Soc.* **2013**, *135*, 17310. (b) Lin, G. Q.; Ding, H. M.; Yuan, D. Q.; Wang, B. S.; Wang, C. *J. Am. Chem. Soc.* **2016**, *138*, 3302. (c) Li, Z. P.; Zhang, Y. W.; Xia, H.; Mu, Y.; Liu, X. M. *Chem. Commun.* **2016**, *52*, 6613. (d) Ding, S. Y.; Dong, M.; Wang, Y. W.; Chen, Y. T.; Wang, H. Z.; Su, C. Y.; Wang, W. *J. Am. Chem. Soc.* **2016**, *138*, 3031.

5 (a) Wan, S.; Guo, J.; Kim, J.; Ihee, H.; Jiang, D. L. *Angew. Chem., Int. Ed.* **2008**, *47*, 8826. (b) Colson, J. W.; Woll, A. R.; Mukherjee, A.; Levendorf, M. P.; Spitler, E. L.; Shields, V. B.; Spencer, M. G.; Park, J.; Dichtel, W. R. *Science* **2011**, *332*, 228. (c) Dogru, M.; Handloser, M.; Auras, F.; Kunz, T.; Medina, D.; Hartschuh, A.; Knochel, P.; Bein, T. *Angew. Chem., Int. Ed.* **2013**, *52*, 2920.

6 (a) Tilford, R. W.; Mugavero, S. J.; Pellechia, P. J.; Lavigne, J. J. *Adv. Mater.* **2008**, *20*, 2741. (b) Spitler, E. L.; Dichtel, W. R. *Nat. Chem.* **2010**, *2*, 672. (c) Dogru, M.; Sonnauer, A.; Gavryushin, A.; Knochel, P.; Bein, T. *Chem. Commun.* **2011**, *47*, 1707. (d) Spitler, E. L.; Colson, J. W.; Uribe-Romo, F. J.; Woll, A. R.; Giovino, M. R.; Saldivar, A.; Dichtel, W. R. *Angew. Chem., Int. Ed.* **2012**, *51*, 2623. (e) Calik, M.; Auras, F.; Salonen, L. M.; Bader, K.; Grill, I.; Handloser, M.; Medina, D. D.; Dogru, M.; Lobermann, F.; Trauner, D.; Hartschuh, A.; Bein, T. *J. Am. Chem. Soc.* **2014**, *136*, 17802.

7 (a) El-Kaderi, H. M.; Hunt, J. R.; Mendoza-Cortes, J. L.; Cote, A. P.; Taylor, R. E.; O'Keeffe, M.; Yaghi, O. M. *Science* **2007**, *316*, 268. (b) Wan, S.; Guo, J.; Kim, J.; Ihee, H.; Jiang, D. L. *Angew. Chem., Int. Ed.* **2009**, *48*, 5439.

8 (a) Kuhn, P.; Antonietti, M.; Thomas, A. *Angew. Chem., Int. Ed.* **2008**, *47*, 3450. (b) Bojdys, M. J.; Jeromenok, J.; Thomas, A.; Antonietti, M. *Adv. Mater.* **2010**, *22*, 2202.

9 (a) Beaudoin, D.; Maris, T.; Wuest, J. D. *Nat. Chem.* **2013**, *5*, 830. (b) Nath, B.; Li, W. H.; Huang, J. H.; Wang, G. E.; Fu, Z. H.; Yao, M. S.; Xu, G. *CrystEngComm*, **2016**, *18*, 4259.

10 (a) Fang, Q. R.; Zhuang, Z. B.; Gu, S.; Kaspar, R. B.; Zheng, J.; Wang, J. H.; Qiu, S. L.; Yan, Y. S. *Nat. Commun.* **2014**, *5*, 4503. (b) Fang, Q. R.; Wang, J. H.; Gu, S.; Kaspar, R. B.; Zhuang, Z. B.; Zheng, J.; Guo, H. X.; Qiu, S. L.; Yan, Y. S. *J. Am. Chem. Soc.* **2015**, *137*, 8352.

11 (a) Uribe-Romo, F. J.; Hunt, J. R.; Furukawa, H.; Klock, C.; O'Keeffe, M.; Yaghi, O. M. *J. Am. Chem. Soc.* **2009**, *131*, 4570. (b) Kandambeth, S.; Mallick, A.; Lukose, B.; Mane, M. V.; Heine, T.; Banerjee, R. *J. Am. Chem. Soc.* **2012**, *134*, 19524. (c) Zhang, Y. B.; Su, J.; Furukawa, H.; Yun, Y. F.; Gandara, F.; Duong, A.; Zou, X. D.; Yaghi, O. M. *J. Am. Chem. Soc.* **2013**, *135*, 16336. (d) Cai, S. L.; Zhang, Y. B.; Pun, A. B.; He, B.; Yang, J. H.; Toma, F. M.; Sharp, I. D.; Yaghi, O. M.; Fan, J.; Zheng, S. R.; Zhang, W. G.; Liu, Y. *Chem. Sci.* **2014**, *5*, 4693. (e) Zhou, T. Y.; Xu, S. Q.; Wen, Q.; Pang, Z. F.; Zhao, X. *J. Am. Chem. Soc.* **2014**, *136*, 15885. (f) Dalapati, S.; Addicoat, M.; Jin, S. B.; Sakurai, T.; Gao, J.; Xu, H.; Irle, S.; Seki, S.; Jiang, D. L. *Nat. Commun.* **2015**, *6*, 7786. (g) Zhu, Y. L.; Wan, S.; Jin, Y. H.; Zhang, W. *J. Am. Chem. Soc.* **2015**, *137*, 13772. (h) Pang, Z. F.; Xu, S. Q.; Zhou, T. Y.; Liang, R. R.; Zhan, T. G.; Zhao, X. *J. Am. Chem. Soc.* **2016**, *138*, 4710. (i) Liu, Y. Z.; Ma, Y. H.; Zhao, Y. B.; Sun, X. X.; Gandara, F.; Furukawa, H.; Liu, Z.; Zhu, H. Y.; Zhu, C. H.; Suenaga, K.; Oleynikov, P.; Alshammari, A. S.; Zhang, X.; Terasaki, O.; Yaghi, O. M. *Science* **2016**, *351*, 365. (j) Xu, S. Q.; Zhan, T. G.; Wen, Q.; Pang, Z. F.; Zhao, X. ACS *Macro Lett.* **2016**, *5*, 99.

12 (a) Uribe-Romo, F. J.; Doonan, C. J.; Furukawa, H.; Oisaki, K.; Yaghi, O. M. *J. Am. Chem. Soc.* **2011**, *133*, 11478. (b) Bunck, D. N.; Dichtel, W. R. *J. Am. Chem. Soc.* **2013**, *135*, 14952.

13 Wan, G.; Fu, Y. A.; Guo, J. N.; Xiang, Z. H. *Acta Chim. Sinica* **2015**, 73, 557.

14 (a) Fujita, M.; Kwon, Y. J.; Sasaki, O.; Yamaguchi, K.; Ogura, K. *J. Am. Chem. Soc.* **1995**, *117*, 7287. (b) Zaworotko, M. J. *Chem. Commun.* **2001**, 1. (c) Wen, L. L.; Dang, D. B.; Duan, C. Y.; Li, Y. Z.; Tian, Z. F.; Meng, Q. J. *Inorg. Chem.* **2005**, *44*, 7161.

15 Feng, X. A.; Chen, L.; Dong, Y. P.; Jiang, D. L. *Chem. Commun.* **2011**, *47*, 1979.

16 (a) Gong, Y. N.; Meng, M.; Zhong, D. C.; Huang, Y. L.; Jiang, L.; Lu, T. B. *Chem. Commun.* **2012**, *48*, 12002. (b) Huang, Y. L.; Gong, Y. N.; Jiang, L.; Lu, T. B. *Chem. Commun.* **2013**, *49*, 1753.

17 (a) An, J. Y.; Geib, S. J.; Rosi, N. L. *J. Am. Chem. Soc*. **2010**, *132*, 38. (b) Zeng, Y. F.; Zou, R. Q.; Zhao, Y. L. *Adv. Mater*. **2016**, *28*, 2855.

18 Rabbani, M. G.; El-Kaderi, H. M. *Chem. Mater.* **2011**, *23*, 1650.

19 Wei, H.; Chai, S. Z.; Hu, N. T.; Yang, Z. Wei, L. M.; Wang, L. *Chem. Commun.* **2015**, *51*, 12178.

Table of Contents